Analytical study to minimize the engine exhaust emissions and safe knock limit of CNG powered four-stroke SI engine

Jeewan V. Tirkey, H.N. Gupta, S.K. Shukla

Mechanical Engineering Department, Institute of Technology, Banaras Hindu University, Varanasi-221005, India.

Abstract

In this paper, theoretical analysis has been done to minimise engine emissions and safe knock limit by changing some operational and design parameters such as equivalence ratio, spark plug location, compression ratio, and cylinder diameter by using computer simulation model. For this purpose a zero dimensional knock model, two zone combustion model(one in front and one behind the flame front), and gas dynamic model have been incorporated. Subsequently, the Nitric Oxide exhaust emission concentrations have been predicted by using the rate kinetic model in the power cycle and along the exhaust pipes. Furthermore, Carbon Monoxide is computed under chemical equilibrium condition and then empirical adjustment is made for kinetic behaviours based upon experimental results. It is inferred that the value of cylinder pressure data, BMEP, BSFC obtained by using computer simulation model based on theoretical analysis are in closer agreement with those which are obtained by previous studies.

Keywords: Two-zone combustion, Onset knock limit, Percentage heat loss, Spark plug location, Cylinder diameter by stroke ratio.

1. Introduction

To meet the twin problems of fuel oil scarcity and air pollution caused by growing use of petroleum fuels, an alternative renewable clean burning fuel CNG has been explored, as a most prominent eco-friendly fuel for use in SI engine vehicles. CNG is a promising alternative fuel to meet strict engine regulation in many countries.

CNG powered engine offers certain advantages e.g. clean combustion (no lead or sulphur compound) due to high H/C ratio, does not contaminate and dilute the engine oil which forms no deposits on spark plug. It also offers advantage over gasoline in terms of its low density and ready miscibility with air, high knock resistance (octane number 120-130), lean burning capability. Its results in smooth start during cold season. However, due to lack of modification in available engines including supply of conversion kits, it is difficult to fully utilize the above properties of CNG powered engine to enhance the performance.

The relative amounts of various pollutants depend on fuel composition (especially fuel –air equivalence ratio), engine design and operating conditions. Many authors[1-3] found that the leaner mixtures give lower quantities of CO and NO, but if the mixture is made too lean the engine may misfire, giving rise to higher HC emissions. They also suggested that for obtaining maximum power the engine needs to

operate near stoichiometric (slightly rich), while the best economy is obtained with a mixture somewhat leaner than stoichiometric.

Emission modeling is essential for the sound theoretical understanding of the mechanisms for pollutants formation. The pollutant formation processes are intimately linked with the primarily fuel combustion process directly through environmental conditions created by these reactions. A simple estimation of the concentration values of various products of combustion is possible assuming chemical equilibrium. However, the concentrations of the pollutants in the exhaust tail pipe of ICE differ from values estimated using chemical equilibrium conditions. Thus the detailed chemical mechanisms by which these pollutants form and the kinetics of these processes are important in estimating emission levels. At the same time, both flow rate and concentrations of each pollutant significantly affect mass emissions. The emission modeling therefore is a complex art involving fluid mechanics and reaction kinetics. Benson-Horlock et al. [2] reported one of the best technique to calculate 12 numbers of product species during equilibrium condition. This technique has been greatly used by many researchers [4-8]. Furthermore, Agarwal et al. [9, 10] have used detailed chemical kinetics mechanism which consisted of 22 species and 104 elementary reactions with KIVA-3 code in their engine modeling.

In engine emission species, specially NO formation, there are many reaction mechanisms proposed by different authors namely Heywood [1], Horlock-Benson [2], Millar et al. [11]: Zeldovich (2 reactions), Extended Zeldovich (3 reactions), super extended Zeldovich (67 reactions) and Lavoie (7 reactions). These equations depend upon the engine operating conditions and accuracy of predictions. Similarly, CO concentrations in exhaust gases are recognized to be kinetically controlled, because CO concentrations are lower than the maximum value measured within the combustion chamber but higher than the corresponding equilibrium value. For this, Benson2, Sher et al. [12] introduced COFAC factor, used to predict CO concentrations, which lies between the peak and exhaust equilibrium values. The more detailed information concerning pollution formation mechanism and their chemical kinetic rate of carbon monoxides, organic compounds, and particulates are adequately discussed in the book of: Horlock-Benson [2], Heywood [1], Turns [13]. Along with reduction of engine emission, the efficiency and power of the engine are also equally important.

Combustion knock has long been one of the major barriers in the development of spark ignition engine for increased efficiency or improved fuel tolerance. Checkel and Dale [14], Chun et al. [15], investigated experimentally and computationally knock characteristics, such as intensity, percentage & occurrence crank angle from pressure and vibration signal using different analysis methods e.g. band pass filter, third derivative and step method . It was also reported that the vibration signal is more useful among these methods.

Heywood [1], Chun et al. [15], Moses et al. [16], Checkel and Dale [14], By A et al. [17], König G et al. [18], Ferguson et al. [3] reported that the knock is an acoustic phenomenon produced by the auto ignition of the unburned gas in front of flame regime called end-gas. They also reported that the thermal efficiency is directly related to the compression ratio, and engine knock occurs more easily if the compression ratio is increased. In order to fully understand the knock phenomenon and to find possible way to avoid knock phenomenon, Moses [16], and Soylu and Gerpen [19] discussed the categories of knocking sub-model:

    (1) Single zone zero dimensional model (Global model).
    (2) Multi zone model (Burned and Unburned).
    (3) Quasi dimensional model (neglecting the transverse variation in the gas flow field).
    (4) Multidimensional model (real gas dynamic flow, detailed kinetic model, which contains several hundred reactions).

They also reported that, the simplest and fastest way to model engine processes and gas auto ignition is using a zero dimensional model with estimated initial conditions at intake valve closing and combining it with global auto-ignition model.

Liberman [20] analyzed these models and inferred that the fuel conditions are described by the system of ordinary differential equations that include terms corresponding to adiabatic compression: the temperature rise due to exothermic reactions and energy losses to the cylinder walls.

Livengood and Wu [21] developed the first published ignition correlation for SI engine, which was integrated form of an empirical model for onset occurrence based on ignition delay. The pressure and temperature histories of a fired engine are used to determine knock onset. The most extensively tested correlation for ignition delay is that proposed by Douaud and Eyzat [22] to determine the knock resistance. The pre-exponential parameter was based on the Octane number of fuel and the end gas

temperature. This model has been used as base by many researcher [1, 6, 23-25] by changing its constants in their own Knock model for different fuel and engine design. The present work involves a theoretical approach to develop a computational model of combustion in SI engine in order to understand auto-ignition mechanism including knock phenomenon and way to reduce it. Also the validation of model is being compared by experimental data provided by Baruah [2], Aslam [26] and Ma [27].

2. Computational model

The present model which consists of two main domains (1) Inlet and exhaust domain and (2) cylinder domain, formally named as General simulation model (GENSIM).

The inlet domain includes the inlet pipes, carburetor, inlet manifold, and inlet valves. On the other side, the exhaust domain which includes exhaust valves, exhaust manifold and exhaust pipes.

In the pipe calculation of multi-cylinder engine, gas dynamic effect in manifold systems is modeled by using unsteady compressible hyperbolic partial differential equations. These equations contain heat transfer, wall friction, area change in pipe, entropy gradient and empirical constants which are used to determine boundary conditions at pipe junctions, valves, and valve ends. These equations are transferred into set of ordinary differential equations by applying method of characteristics (MOC) and are solved by finite difference method (FDM). In which the compatibility relationships between local fluid velocity (u) and sonic velocity (a) are expressed in terms of Riemann variables, which are constant along the position characteristics [2, 28]. Then the equations are solved numerically by using rectangular grid in the flow direction (x) and time (t). Finally, this calculates pressure wave, temperature variation, and exhaust emission concentration along the exhaust pipes.

In the cylinder domain, which takes into account the various type of processes occurring inside the engine cylinder e.g. compression, ignition, ignition delay, turbulent combustion, expansion and exhaust. The objective of this model in this domain is to calculate instantaneous pressure, unburned and burned temperature, burned and unburned mass, 12 exhaust emission concentrations with respect to crank angle and total heat transfer, power cycle work out put, and knock onset index.

2.1 Two zone combustion model

Thermodynamic combustion process is modeled as turbulent flame propagation process with two zones (burned and unburned). The first law and state of thermodynamic equations are expressed in differential form and integrated by Runge-Kutta method. The equations for the pressure and temperature of the burned and unburned mixture are:

$$\frac{dT_m}{d\alpha} = \frac{V_m}{m_m c_{p_m}} * \frac{dp}{d\alpha} + \frac{1}{m_m c_{p_m}} * \frac{dQ_m}{d\alpha} \tag{1}$$

$$\frac{dT_p}{d\alpha} = \frac{p}{m_p R_p}\left[\frac{dV}{d\alpha} - \left(\frac{R_p T_p}{p} - \frac{R_m T_m}{p}\right)\frac{dm_p}{d\alpha} - \frac{R_m V_m}{pc_{p_m}}\frac{dp}{d\alpha} - \frac{R_m}{pc_{p_m}}\frac{dQ_m}{d\alpha} + \frac{Vdp}{pd\alpha}\right] \tag{2}$$

$$\frac{dp}{d\alpha} = \left[\begin{array}{l}\left[\left(1 + \frac{c_{v_m}}{R_p}\right)p\frac{dV}{d\alpha} + \left\{(u_p - u_m) - c_{v_p}\left(T_p - \frac{R_m}{R_p}T_m\right)\right\}\frac{dm_p}{d\alpha} + \right.\\ \left.\left\{\frac{c_{v_m}}{c_{p_m}} - \frac{c_{v_p}}{R_p}\frac{R_m}{c_{p_m}}\right\}\frac{dQ_m}{d\alpha} - \frac{dQ}{d\alpha}\right]\end{array}\right] \Bigg/ \left[\frac{c_{v_p}}{c_{p_m}}\frac{R_m}{R_p}V_m - \frac{c_{v_m}}{c_{p_m}}V_m - \frac{c_{v_p}}{R_p}V\right] \tag{3}$$

.

where T is the temperature (K), p is the pressure (N/m^2), Q is the total heat flux, m is the mass (kg), c_p is the specific heat of gas at constant pressure (kJ/kgK), c_v is the specific heat of gas at constant volume (kJ/kgK), V is the volume (m^3), R is the gas constant (kJ/kgK), u is the specific internal energy (kJ/kg), α is the crank angle(degree). The suffix (m) for the unburned, (p) for the product (burned), and (w) for the wall.

The heat transfer from both the burned and unburned gases is calculated by using Annand's convective heat transfer equation. Theoretically combustion should terminate when $V_m \to 0$: In this numerical solution, it is assumed to terminate at the beginning of the time step where the current value of V_m is just negative. The details are given in reference [2, 7, 8].

2.2 Heat transfer to the wall
The heat transfer rate from gas to wall is calculated by Annand's equation [29].

$$\frac{q}{F} = a\frac{k_q}{D} * \left(R_e\right)^b * \left(T_m - T_w\right) + c\left(T_m^4 - T_w^4\right)$$ (4)

where k_q is the thermal conductivity ($k_q = \dfrac{c_p \mu}{0.7}$), F is the area (m²), D is the cylinder bore diameter (m),

Re is the Reynolds number ($= \dfrac{\rho D S_m}{\mu}$, where S_m is mean piston speed, density ρ, and viscosity μ),

and a, b and c are constants (a = 0.4, b = 0.7, c = 4.3 * 10⁻⁹).

2.3 Flame speed
The turbulent flame front speed, u_T (m/s), is calculated by following equation given by Klimov which is taken from references [13, 30].

$$u_T = 3.5\left(u'\right)^{0.3} + \left(u_l\right)^{0.7}$$ (5)

where u' is root mean square(rms) turbulent velocity, calculated by modification of turbulence model used by Verhelst [31] in which the integral length scale is kept constant at one-fifth the minimum clearance height, and the rms turbulence velocity linearly decreases according to;

$$u' = u'_{TDC}[1 - 0.5(\theta - 360)/45]$$ (6)

where u'_{TDC} is rms turbulent velocity at TDC, taken to be around 0.5 times [1] (0.57taken) of the mean piston speed, θ is the crank angle (360⁰ at TDC of compression). u_l (cm/s) is laminar flame speed, which is calculated from the expression given by Liao [32];

$$u_l = u_{l0}\left\{\frac{T_u}{T_{u0}}\right\}^{\alpha_T} \left\{\frac{P_u}{P_{u0}}\right\}^{\beta_p}$$ (7)

where the reference pressure and temperature are $P_{u0} = 0.1$ MPa, and $T_{u0} = 300$K, respectively. u_{l0} (cm/s) is the burning velocity at P_{u0} and T_{u0}. α_T And β_T as well as u_{l0}, are functions of equivalence ratio ($\varnothing$), and are given by:

$$u_{l0} = -177.43\varnothing^3 + 340.77\varnothing^2 - 123.66\varnothing - 0.2297$$ (8)

$$\alpha_T = 5.75\varnothing^2 - 12.15\varnothing + 7.98,$$

$$\beta_p = -0.925\varnothing^2 + 2\varnothing - 1.473$$

2.4 Knock model
At present, it is postulated that the high temperature and pressure caused in the front of flame regime called end-gas during the combustion process cause part or all of it to ignite spontaneously [1-4].
A simple model for knock is to assume that it occurs if there is sufficient time (induction or autoignition time) for enough of the initiating radicals, or precursors, to be produced [22].
Induction-time correlations are derived by matching an Arrhenius function to measured data on induction or autoignition times, for given fuel-air mixtures over the relevant mixture pressure and temperature

ranges. *Knock integral method* is then proposed by Livengood and Wu [21] by which an ignition delay correlation could be used to determine knock occurrence crank angle (KOCA). The knock integral has the following form;

$$\int_{t=0}^{t_i} \frac{dt}{\tau} = 1 \tag{9}$$

In terms of Crank angle

$$\frac{1}{\tau} \times \frac{1}{0.006N} \int_{\theta_o}^{\theta_i} d\theta = 1 \tag{10}$$

where τ is the induction time at the instantaneous temperature and pressure for the mixture, t (or θ crank angle) is the elapsed time from the start of the end-gas compression process (t=0 or at θ_0 crank angle: after ignition lag), t_i (or θ_i crank angle) is the time of autoignition, and N is the revolutions per minute. Using this concept, the most extensive tested correlation is produced by Douaud and Eyzat [22], which is widely accepted by Heywood [1], Turner et al. [24].

$$\tau = 17.68 \left(\frac{ON}{100}\right)^{3.402} P^{-1.7} \exp\left(\frac{3800}{T}\right) \tag{11}$$

where τ is in milliseconds, *p* is absolute pressure in atmospheres, *T* is in kelvin and *ON* is the octane number of fuel.

2.5 Total friction work for SI engine

The total friction work contains three major components. These components are the *pumping work*, W_p, which is net work per cycle done by the piston on the in-cylinder gases during the inlet and exhaust strokes; *rubbing friction work*, W_{rf}, which is the work per cycle dissipated in overcoming the friction due to relative motion of adjacent components within the engine; and *accessories work*, W_a, which is the work per cycle required to drive the engine accessories, e.g., pumps, fan, generator etc. The total friction work can be expressed as follows:

$$W_{tf} = W_p + W_{rf} + W_a \tag{12}$$

The data of total motored friction mean effective pressure (TFMEP) for several four stroke cycle, four cylinder SI engines between 845 and 2000cm³ displacement, at wide open throttle, as a function of engine speed [33] are well correlated by an equation, which is widely used by Heywood [1] and Abd Alla [34].

$$TFMEP(bar) = 0.97 + 0.15\left(\frac{N}{1000}\right) + 0.05\left(\frac{N}{1000}\right)^2 \tag{13}$$

where N is revolutions per minute.

Thus, the brake mean effective pressure (BMEP) of the standard engine can be found by the following expression:

$$BMEP = IMEP - TFMEP \tag{14}$$

and;

$$\text{Brake Power (BP)} = BMEP \times V_d \times \left(\frac{N}{n_R}\right) \times n_{cyl} \tag{15}$$

where *IMEP* is the indicated mean effective pressure, which is the work delivered to the piston over the compression and expansion stroke, per cycle per unit displacement volume; n_R is the number of revolutions per cycle (=2 for four stroke cycle); n_{cyl}, is the number of cylinder (=4).

2.6 Species formation

Twelve species are considered in the combustion products in the cylinder and in the exhaust. they are : H_2O, H_2, OH, H, N_2, NO, N, CO_2, CO, O_2, and Ar. Properties of mixture at every time step are calculated by using polynomial coefficients of internal energy for these 12 species. These species could reach equilibrium condition if sufficient time is allowed for the reactions to take place under a certain state [1-2]. The details are given in the book of Benson [2], consisting of 7 governing equations.

The formation of Nitric Oxide in an engine combustion chamber is a non equilibrium process. The rate kinetics model based on the seven governing equations for NO formation is considered in the power cycle and along the exhaust pipes based on the theory developed by Lavoie at.el., which is taken from reference [2]. Carbon monoxide is computed under chemical equilibrium condition and then empirical adjustment is made for kinetic behaviours based upon experimental results.

3. Validation

The results of the computational model are verified against the experimental data of the gasoline fueled engine used by Baruah et al. [35], CNG fueled engine by Aslam [26] and Ma Fanhua [27] as shown in Figures 1, 2, and 3 respectively. These figures show that the results predicted by the mathematical model are quite close (within 3%) to the experimental results. The technical data used for power cycle modeling for different engines are given in Table 1.

Figure 1 shows the comparison of computed in-cylinder pressure vs. crank angle diagram for gasoline fueled engine with experimental one during power cycle at fuel-air equivalence ratio of 0.967, 1.084, and 1.173. The computed data closely follow the experimental data except in the vicinity of peak pressure. Figure 2 shows more clearly the comparison of measured and computed peak pressures at different equivalence ratio. The average difference is around 3%. The discrepancy of this peak pressure is caused by the cycle to cycle dispersion, and is due to non-homogeneity of fuel mixture supply in the cylinder in actual case, but theoretical calculations are based on constant homogeneous mixture supply at every cycle. Great deals of experimental research work by Zerves Efthimis [36], Ceviz MA [37] have been done on cyclic dispersion. Many authors [38, 39] suggested that the major source of cycle to cycle variation is due to the variation in the spherical burning area, produced by variation in the position of the wall contact flame center and variation in the laminar flame speed at the spark center. In Figure 3, the experimental and predicted results of NO and CO emission concentrations are compared with the variation of fuel air equivalence ratio.

In Figure 4, the experimental indicated mean effective pressure and corresponding computational results are compared with the variation of fuel-air equivalence ratio.

In Figure 5, the experimental results of cylinder pressure for CNG fueled engine are compared with the present simulation model at the equivalence ratio(ER) of 0.7692. It shows that computed curve follows the experimental pressure curves very closely.

Figure 6, compares the experimental Brake means effective pressures (BMEP) given by Aslam et al. [26] for a CNG fueled engine and the theoretical ones calculated by using the present model. These figures show that computational results are reasonably in good agreement with the measured one. The BMEP maximizes at midrange of engine speed ($\approx$ 3000 RPM). This is due to the friction which increases with increasing engine speed. Another reason of BMEP loss is due to the longer ignition delay and low flame speed of CNG fuel. These factors affect the Brake specific fuel consumption (BSFC). The figure shows that BSFC drops as the engine speed increases in the low speed range and level off at medium speed range and increases towards the high speed range. This is because of the heat losses to the combustion chamber which proportionally increases with decrease in speed. On the other hand BSFC increases due to the friction which increases with increase in engine speed.

It can be seen obviously from these comparisons that the present simulation model is capable to compute accurately the engine performance of SI engine using gasoline or CNG fuel.

Table 1. Technical data of engines for validation

Gasoline

Engine type (SI)	Vauxhall Victor 2000cc (Baruah [34], Benson [2])
Cycle	4 stroke
Cylinder bore	9.53cm
Stroke	6.92cm
Connecting rod length	13.65cm
Compression ratio	8.5
Angle of ignition	33.6^0 bTDC
Valve timing	
evo	114.6^0 aTDC
evc	393.4^0 aTDC
ivo	326.6^0 aTDC
ivc	605.4^0 aTDC
Lower calorific value	44MJ/kg

CNG (Test Engine 1)

Engine type (SI)	Proton Magma (Aslam [26])
Cycle	4 stroke
Cylinder bore	7.55cm
Stroke	8.2cm
Connecting rod length	13.65cm
Compression ratio	9.2
Angle of ignition	40.00 bTDC
Lower calorific value	47.377MJ/kg

CNG (Test Engine 2)

Engine type (SI)	Dongfeng Motor (Ma F [27])
Cycle	4 stroke
Cylinder bore	10.5cm
Stroke	12.0cm
Connecting rod length	19.2cm
Compression ratio	10.5
Angle of ignition	30.00 bTDC
Valve timing	
evo	123.65 aTDC
evc	371.65 aTDC
ivo	341.65 aTDC
ivc	577.65 aTDC
Lower calorific value	47.377MJ/kg
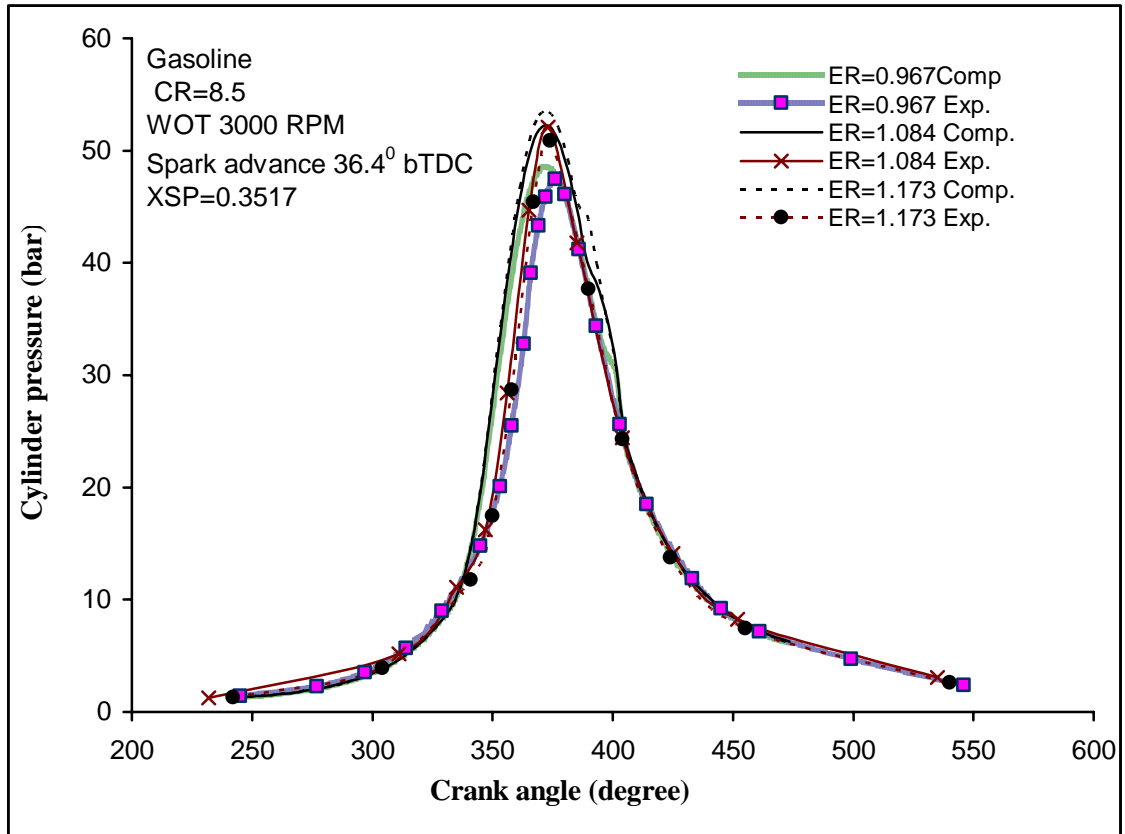
Figure1. Comparison of measured and computed cylinder pressure with crank angle at different equivalence ratio
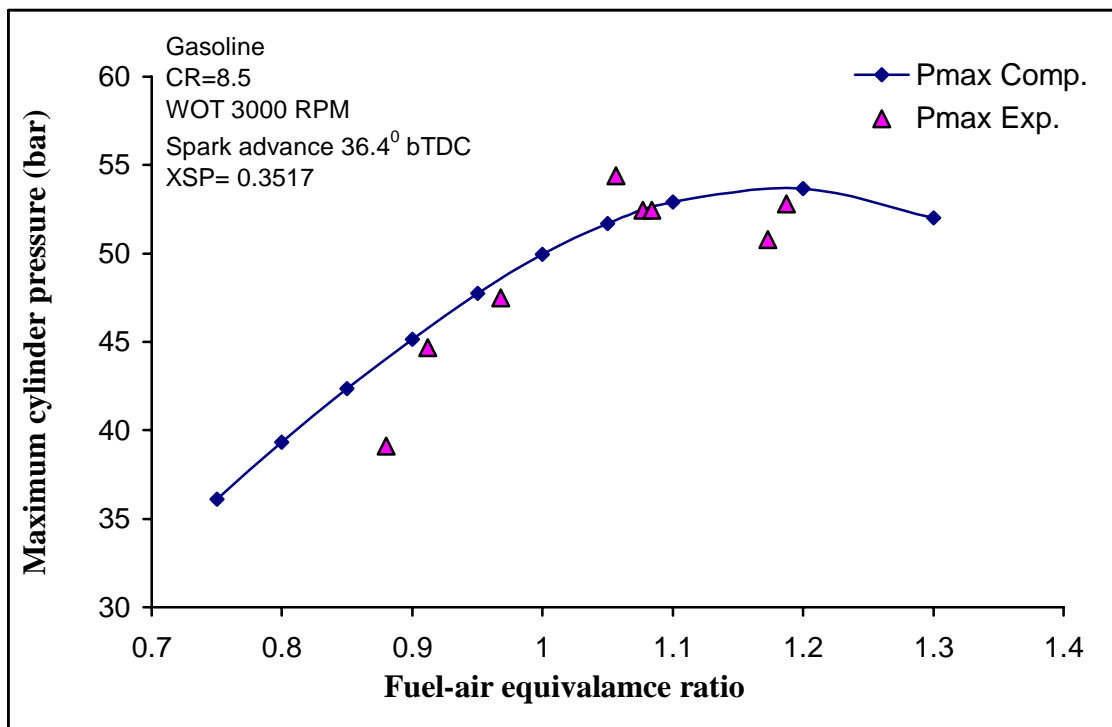
Figure 2. Comparison of measured and computed maximum cylinder pressure
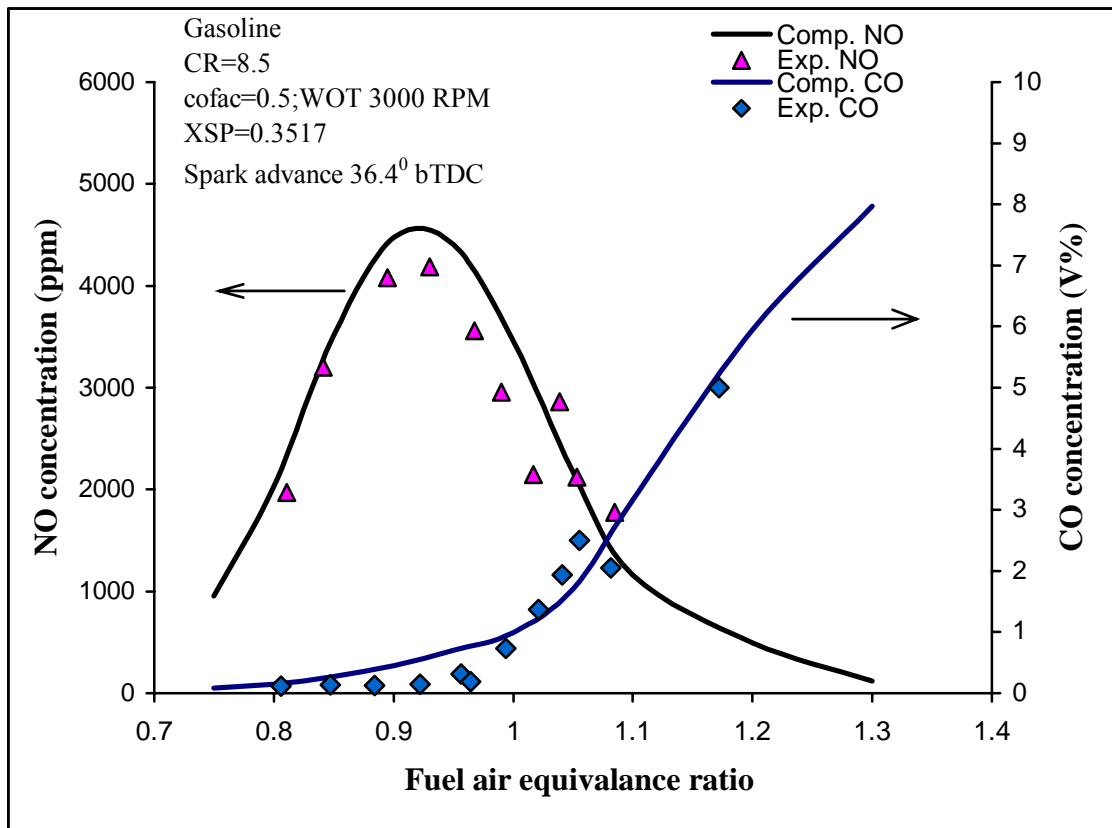
Figure 3. Comparison of measured and computed NO and CO concentration at different fuel-air equivalence ratio
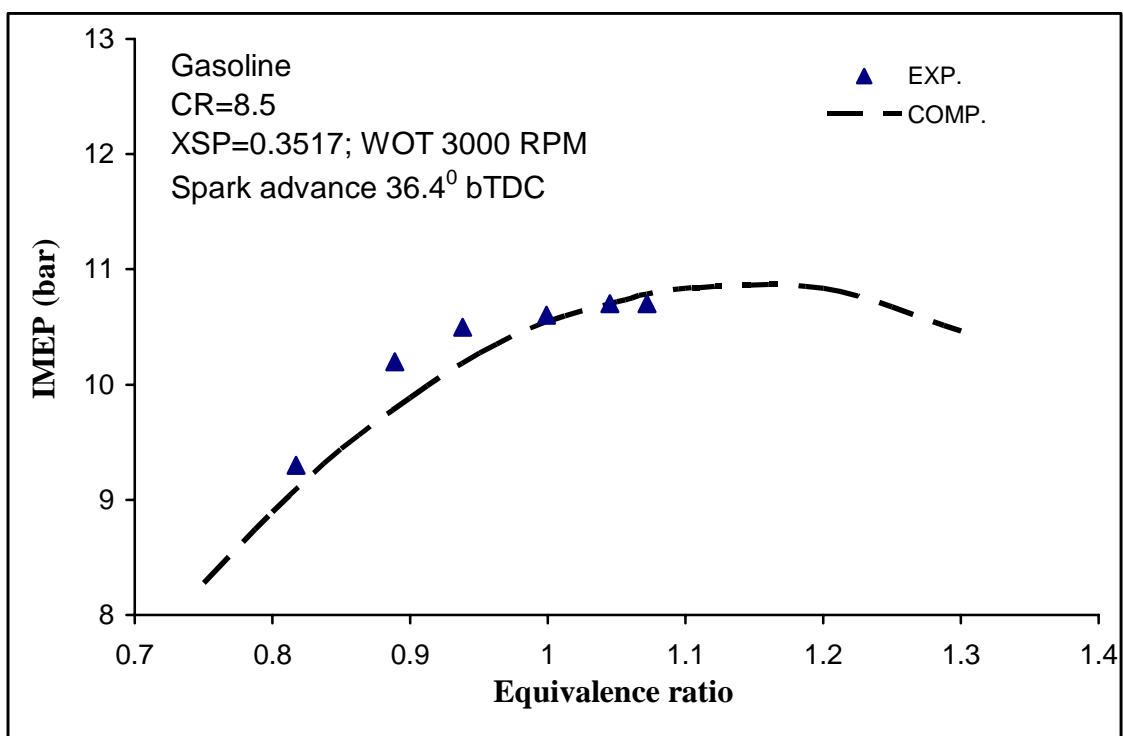
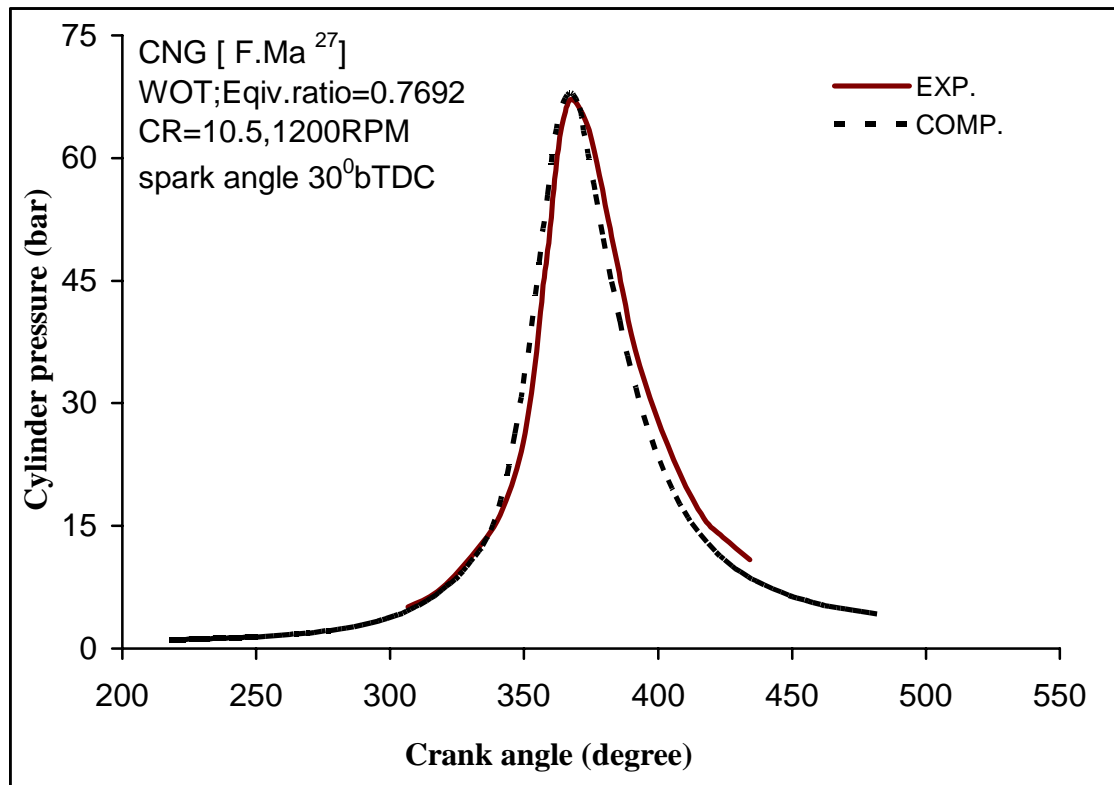Figure 4. Comparison of computed and experimental IMEP with variation of equivalence ratio

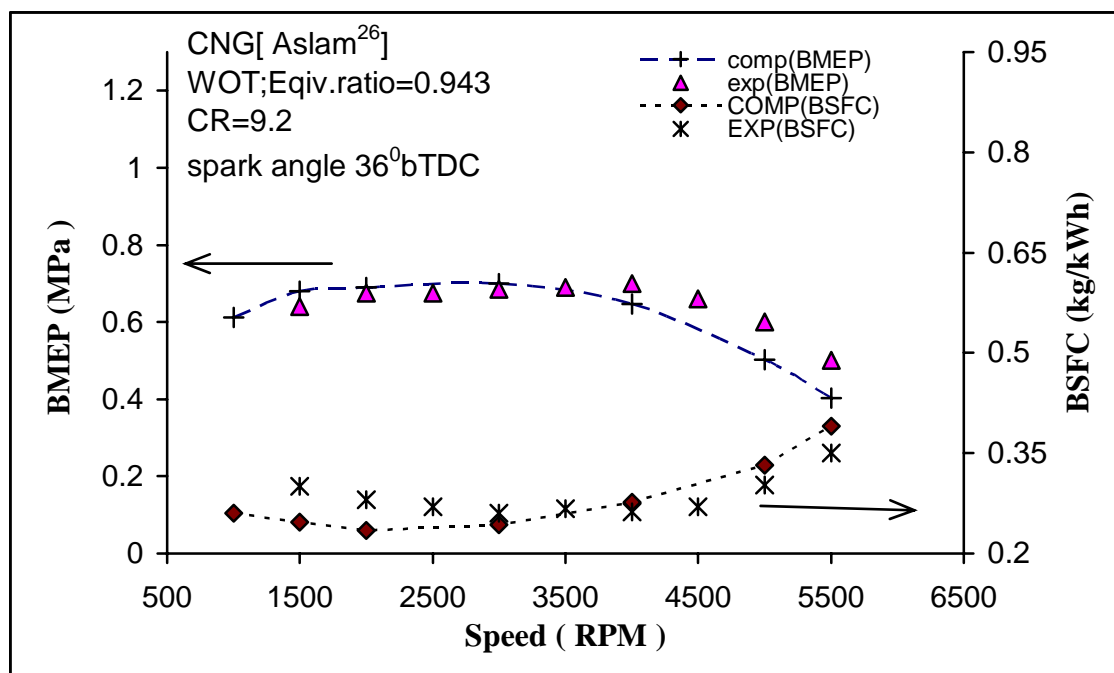Figure 5. Comparison of computed and experimental cylinder pressure with crank angle

Figure 6. Comparison of computed and experimental BMEP and BSFC with the variation of engine speed

4. Results and discussion

Figure 7 shows the effect on in-cylinder pressure development with crank angle at different compression ratio, at 3000 RPM wide open throttle and 36^0 bTDC spark timing. Figure illustrates that, with increase in compression ratio peak pressure increases. This could be more clearly seen in Figure 8. This is

because, the value of pressure and temperature of the mixture during sparking are higher at higher compression ratios and heat release during combustion further increases the pressure and temperature to the higher level. In the same time apparent flame speed increases and consequently combustion duration decreases, this is shown in Figure 9.

The composition of the working mixture influences the rate of combustion and amount of heat evolved. When the mixture is made leaner, it releases less thermal energy resulting in lower flame temperature and hence flame speed reduces. With increase in compression ratio, the clearance volume decreases and a greater portion of spent up gases are exhausted. This means, that there is less dilution of the charge and charge density is greater during the burning process. In addition to this, the temperature of the charge is high at higher compression ratio. Since the heat transfer increases with greater charge density and increased temperature, the flame speed increases. At very lean air /fuel ratio, increasing compression ratio results no significant change in flame speed. The combustion duration decreases with increase of compression ratio, because the maximum cycle gas temperature increases resulting in higher apparent flame speed. These factors greatly affect engine performance.

Figure 10 shows the effect of compression ratio on engine power, IMEP and BMEP, fuel consumption and thermal efficiency. The increase in compression ratio shows the increase in mean effective pressure and engine power, which is due to the higher cylinder gas pressure. The same figure also shows, as compression ratio increases the specific fuel consumption decreases due to improved combustion with higher peak pressure and temperature and due to more scope of expansion work.

Figure 11 shows the effect of compression ratio on CO and NO concentrations at exhaust-valve. It is observed from the figure that as the compression ratio increases the concentrations of CO and NO emission increase by increasing the maximum cycle temperature. In continuation, the effect of compression ratio on CO and NO concentrations with fuel air equivalence ratio are shown in Figure 12. In this figure equivalence ratio and spark timing are adjusted for maximum torque for BMEP data. This also depicts that as compression ratio increases, the concentrations of NO and CO emission level increase due to increase of cylinder temperature as shown in Figure 8.

It can be observed from Figure 10, higher the compression ratio higher is the indicated thermal efficiency. The compression ratio is limited by two practical considerations, namely, material strength and engine knock. Engine heads and blocks have a designed maximum stress, which should not be exceeded, thus limiting the compression ratio. On the other hand, if maximum temperature exceeds the auto-ignition temperature of air-fuel mixture, combustion will occur ahead of the flame, knock occurs due to high rate of pressure rise causes damage to the engine.

Figure 13 shows the onset knock-limited compression ratio as a function of fuel-air equivalence ratio, for two fuels with different octane number. The highest requirement is for slightly rich mixtures; increasing richness and leanness, about this point decreases the octane requirement subsequently. Onset knock limit depends on spark advance as shown in Figure 14: more advance sparking increases the peak pressure of the cycle and therefore increases the pressure and temperature of the end charge resulting shortens delay period (induction/auto ignition time) and increases the tendency to knock.

Figure 15 shows the onset knock-limited compression ratio as a function of equivalence ratio and cylinder diameter. In this figure, XDS value is the ratio of cylinder diameter and fixed stroke length. The figure shows, initially onset knock limit decreases from 0.5 to 0.75 XDS and then increases with increase in XDS value with increase in cylinder diameter. This is because high surface to volume ratio occurs for smaller diameter engine, resulting in higher percentage of heat loss as shown in Figure 16.

The emission of carbon monoxide and nitric oxide also limits the use of higher compression ratio. The concentrations of NO and CO emission depend upon compression ratio as well as spark plug location, which is shown in Figures 17 and 18 respectively. Positioning of spark plug towards centre (XSP=0.125 to 0.5) and increasing compression ratio, NO and CO emission levels increase almost linearly in both the conditions due to temperature increase inside the cylinder.

Figures 19 and 20 depict the effect of compression ratio and cylinder diameter to stroke length ratio (XDS) on NO and CO emission levels at exhaust valve. These figures have been plotted for 0.9434 equivalence ratio, 3000 RPM engine speed and 36^0 bTDC spark timing. These figures illustrate that NO and CO concentration levels increase by increasing XDS value and compression ratio. XDS is the ratio of cylinder diameter and stroke length, where cylinder diameter is changed and stroke length is kept constant. Smaller the value of XDS means smaller cylinder diameter, high surface to volume ratio, resulting in higher percentage of heat loss as shown in Figure 16. Thus low temperature inside the cylinder implies low emission of NO and CO concentrations.
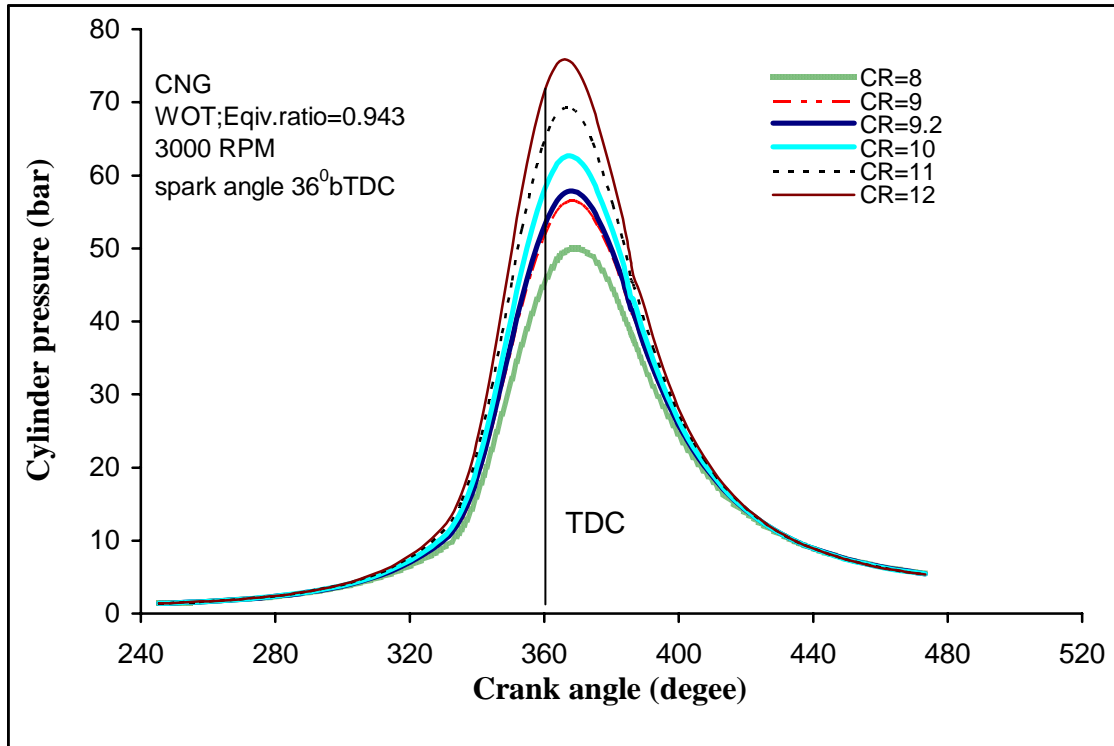
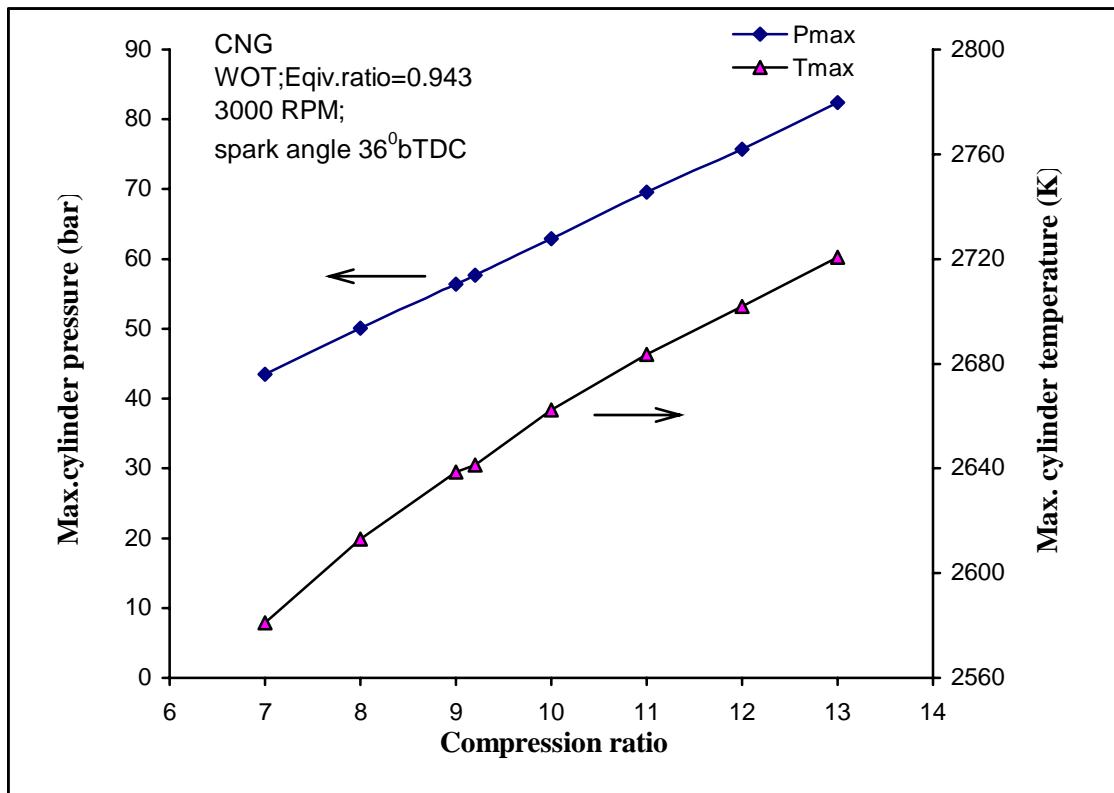Figure 7. Variation of in-cylinder pressure with crank angle at different compression ratio

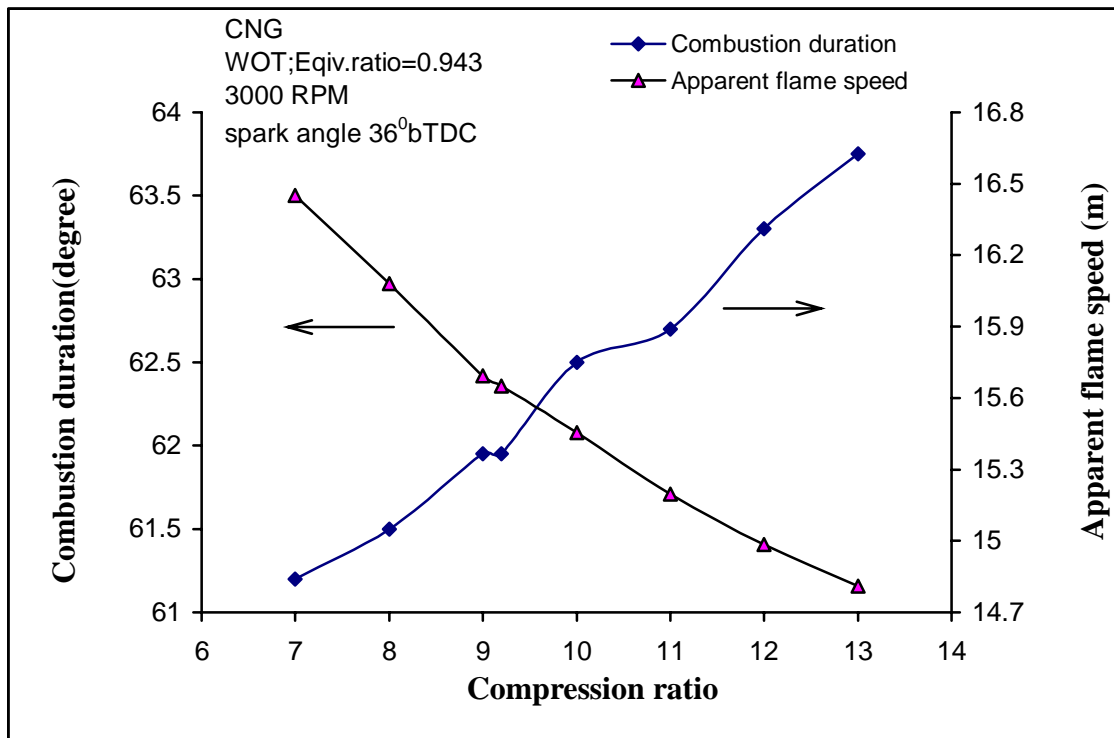Figure 8. Variation of maximum cylinder pressure and temperature with compression ratio

Figure 9. Variation of combustion duration and apparent flame speed at different compression ratio
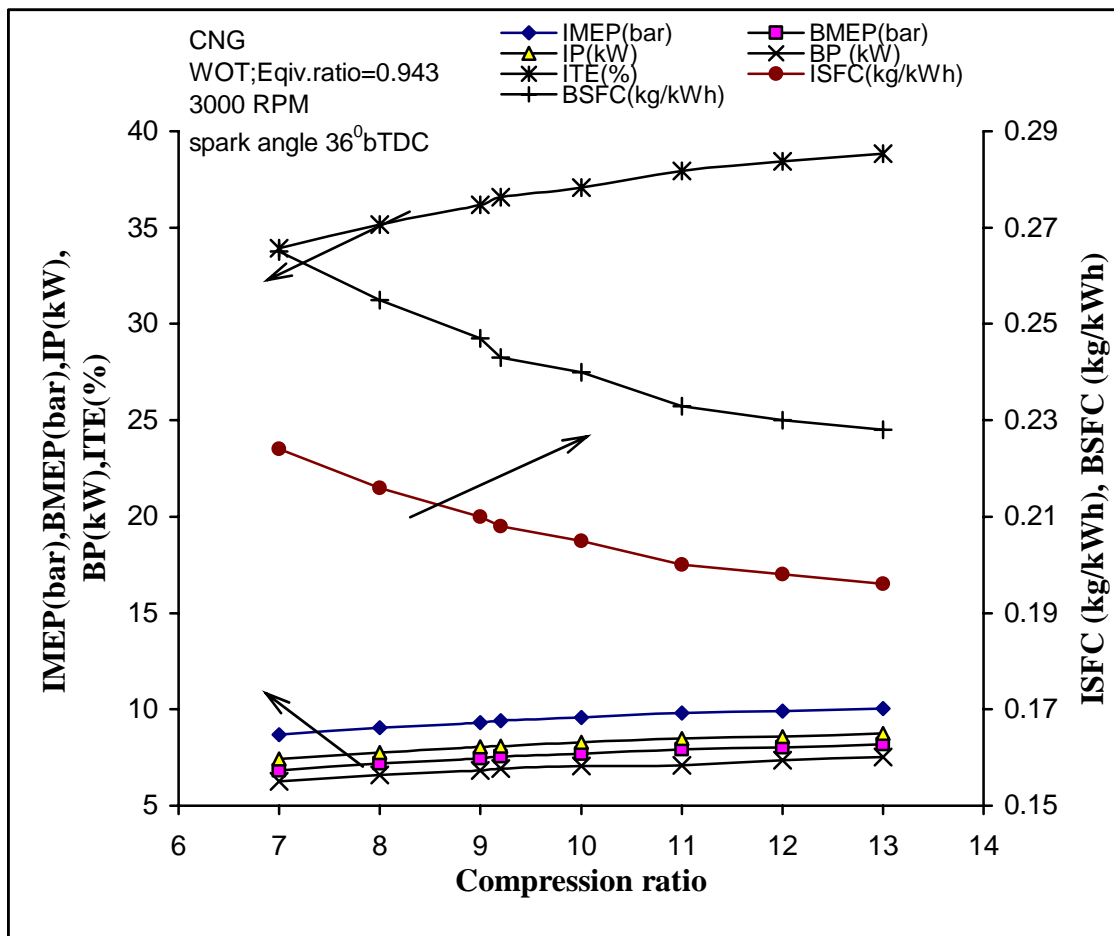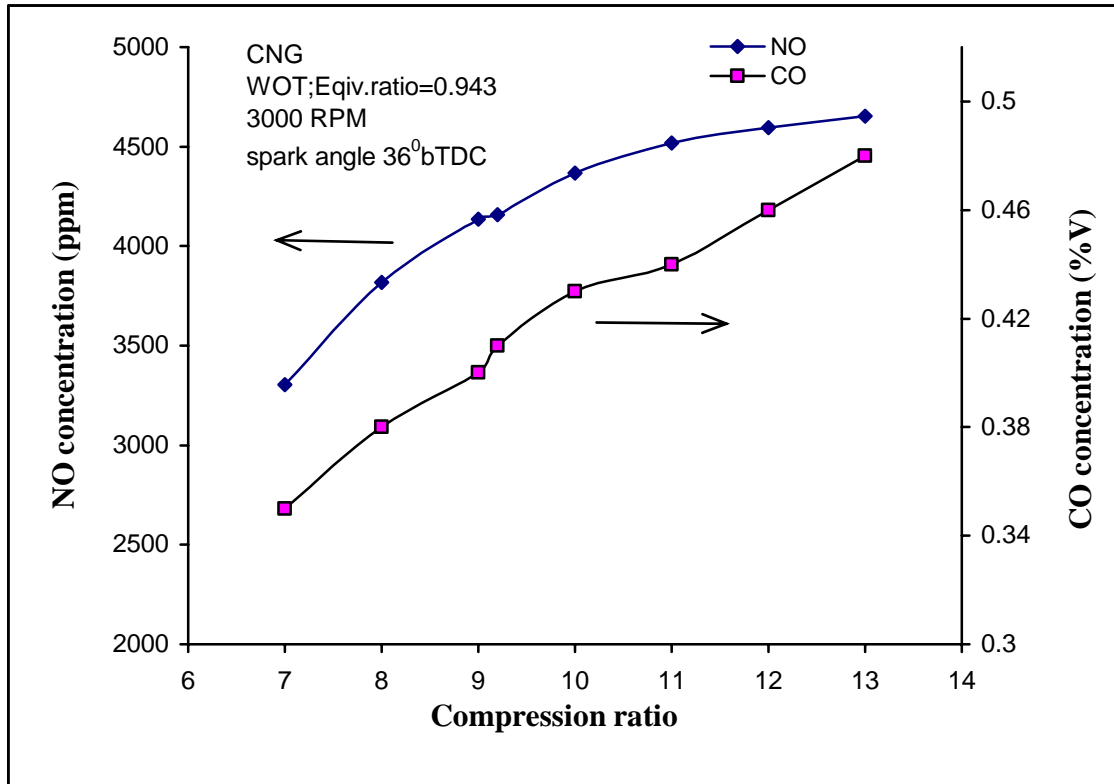

Figure 10. Engine performances vs. compression ratio

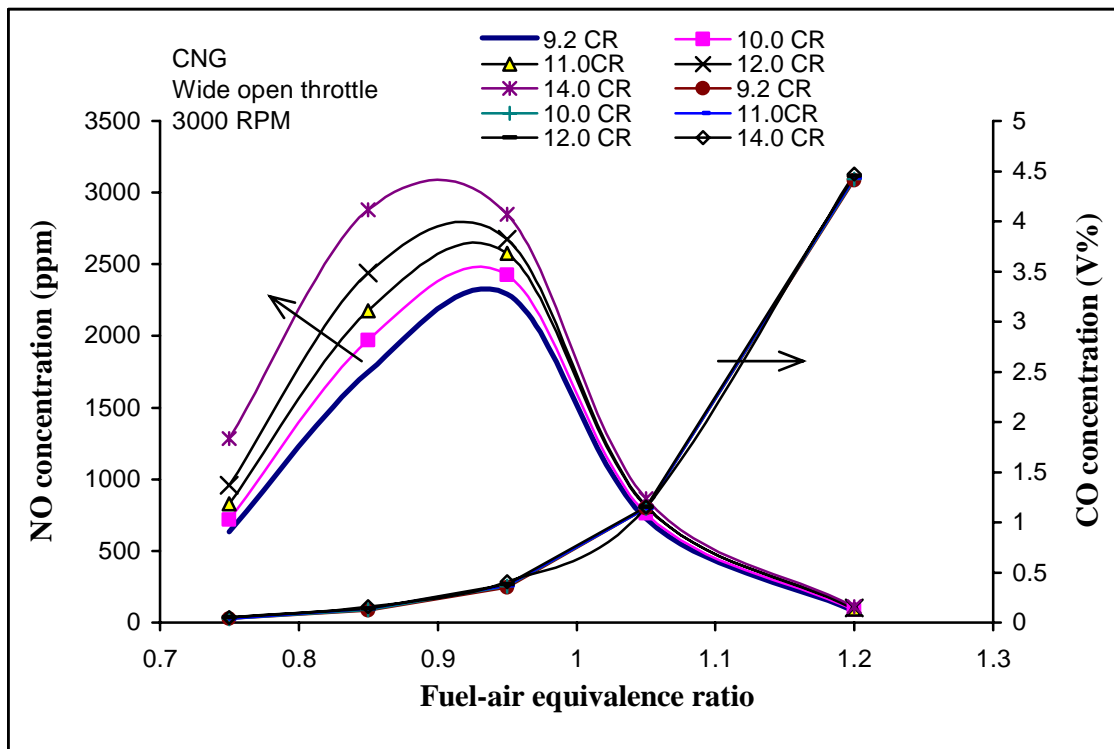Figure 11. Variation of NO and CO concentration with compression ratio variation

Figure 12. Variation of NO and CO concentration vs. equivalence ratio at different CR with MBT condition
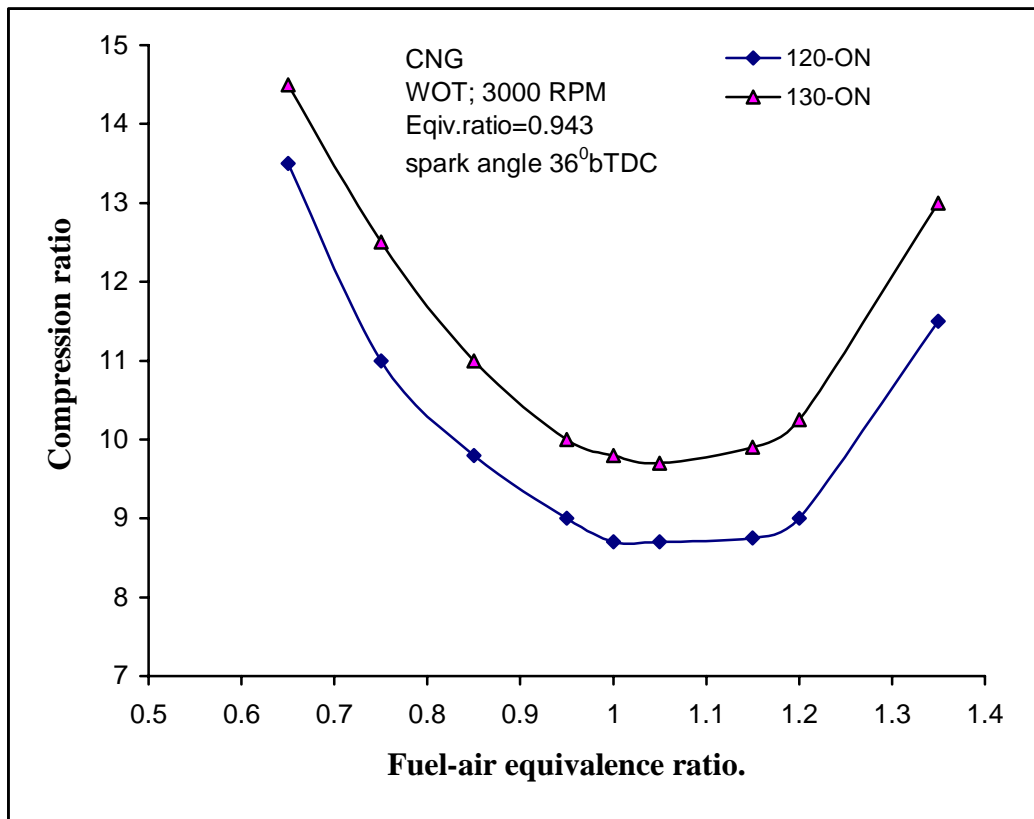
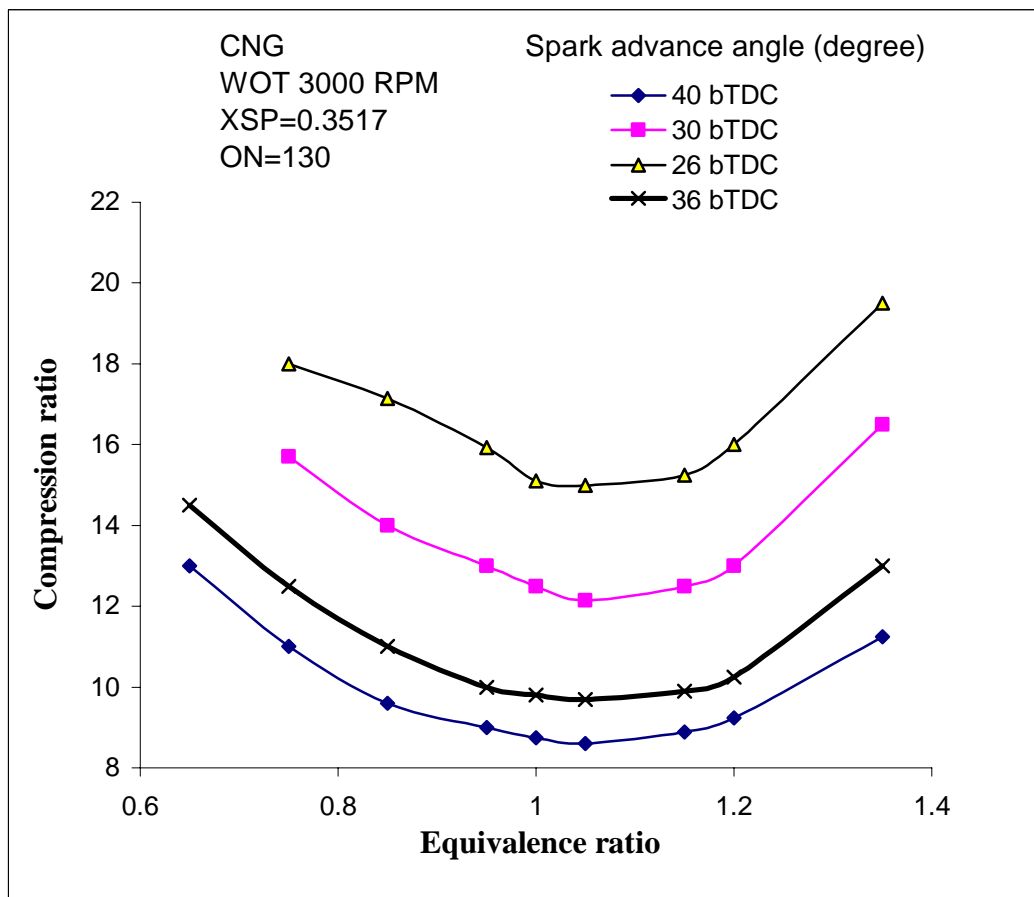Figure 13. Knock limits as function of compression ratio and fuel-air equivalence ratio

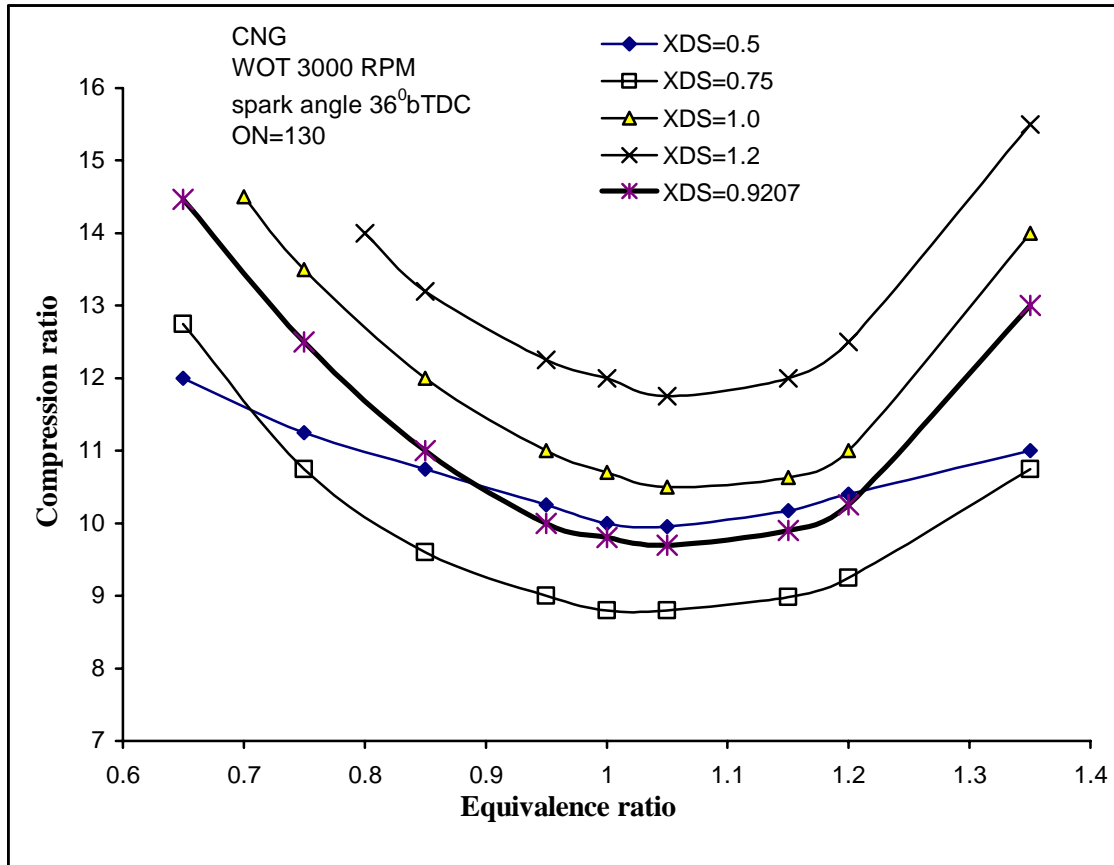Figure 14. Variation of onset knock limit with equivalence ratio and spark advance

Figure 15. Variation of onset knock limit with equivalence ratio and the value of XDS (diameter/stroke)
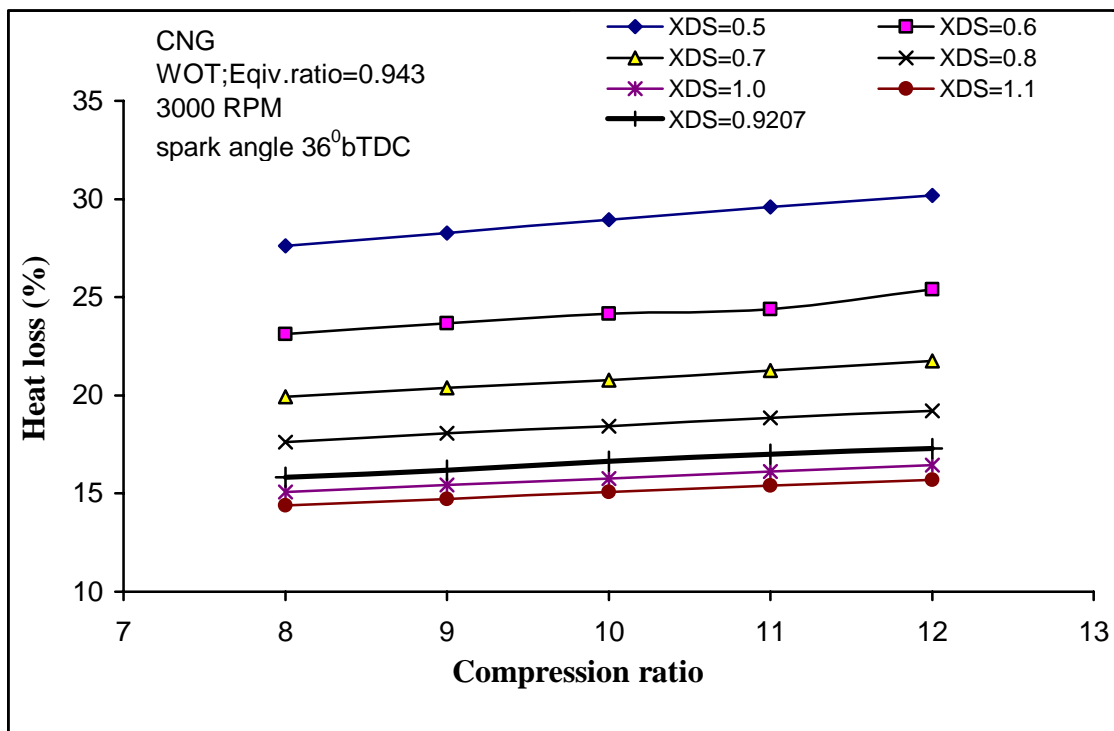

Figure 16. Variation of percentage heat loss during power cycle with compression ratio at different value of XDS
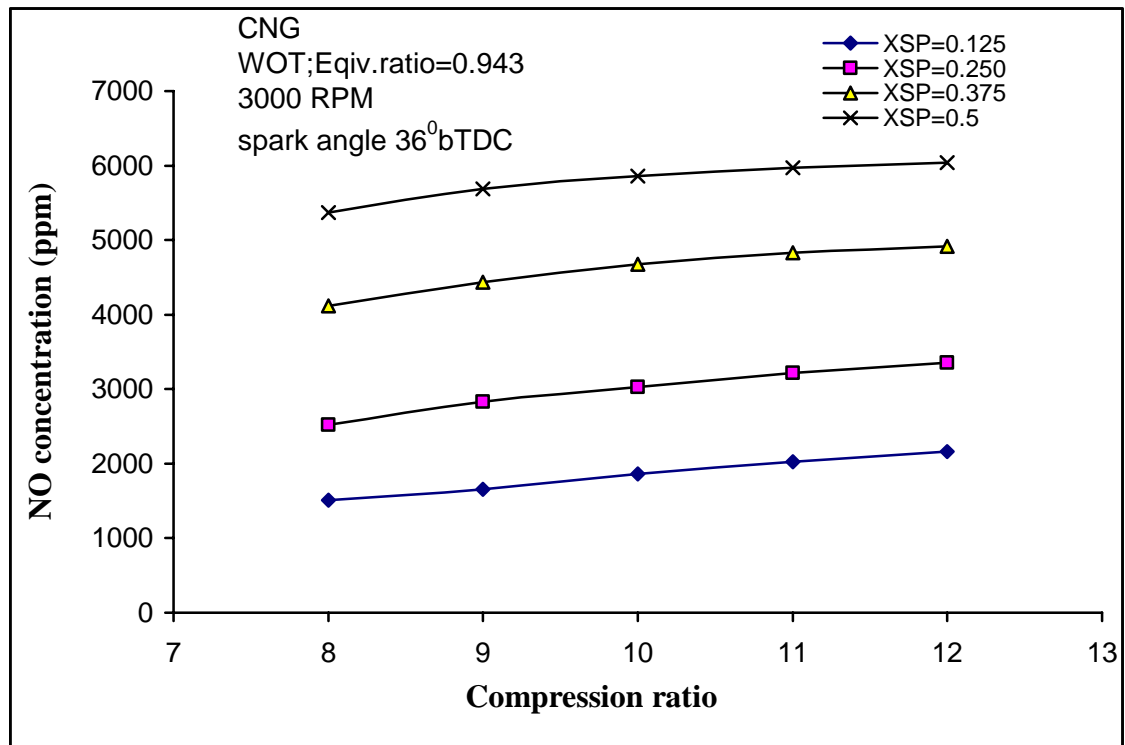
Figure 17. Variation of NO concentration with compression ratio at different spark plug location
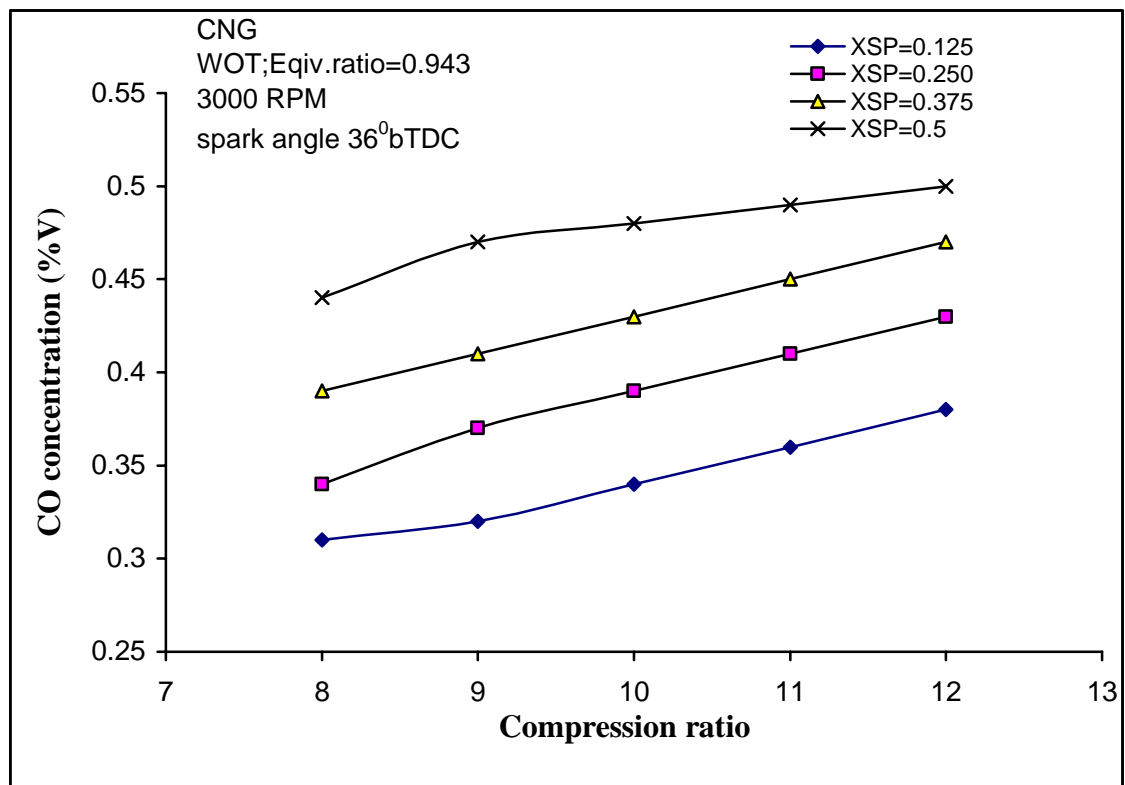

Figure 18. Variation of CO concentration with compression ratio at different spark plug location
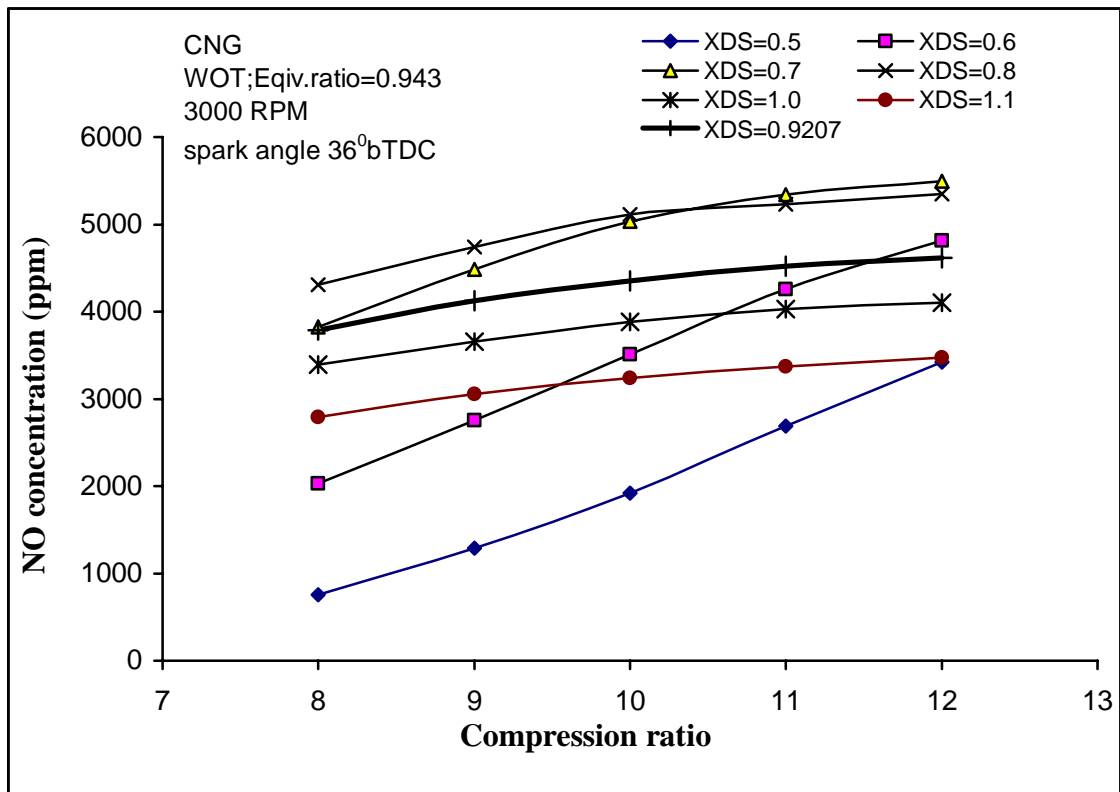
Figure 19. Variation of NO concentration with compression ratio at different value of XDS (diameter /stroke)
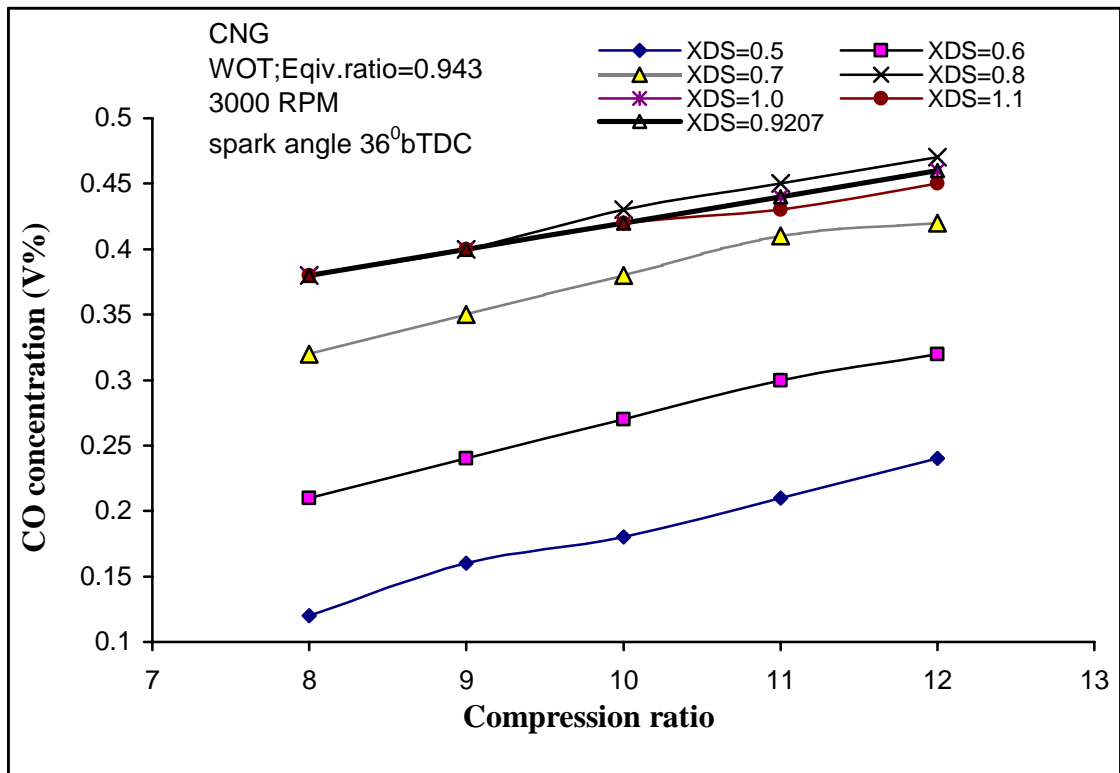

Figure 20. Variation of CO concentration with compression ratio at different value of XDS (diameter/stroke)

5. Conclusion

A general engine simulation GENSIM technique has been developed to model power cycle interfaced with gas dynamic effect of intake and exhaust manifolds of four-cylinder spark ignition engines.

Comparisons between theoretical results obtained from the present computer simulation model and experimental results have been made to confirm for the reliability and accuracy of the present model for predicting performance of SI engine running on gasoline and CNG fuel.

The following conclusions are drawn from the present analytical diagnostics:

1. The CNG fueled SI engine is most efficient when running on stoichiometric or slightly lean (Ø=0.9-1.0) mixture at moderate engine speed (≈ 3000 RPM) and MBT spark timing.
2. Brake power, indicated power and thermal efficiency increase with the increase of compression ratio.
3. The CO emission increases towards rich mixture. NO concentration varies with fuel conditions as it increases at slightly lean stoichiometric mixture (Ø ≈0.9Ø) and reduces toward leaner and richer mixture.
4. The highest requirement of knock limit compression ratio is for slightly rich mixture (Ø=1-1.15), increasing richness on leanness decreases the octane requirement subsequently.
5. Onset knock limit depends on spark advance. An increase in spark advance from the optimized timing increases the tendency to knock, thus retarding has low tendency to knock.
6. It is observed that retarding timing helps to reduce NO_x and knock. Thus retarding timing is preferable from the MBT timing, although some power is lost.
7. Onset knock limit depends upon cylinder bore- to- stroke ratio. Onset knocks decreases from 0.5 to 0.75 XDS and then increases with increase in XDS value.

References

[1]   J.B. Heywood. International combustion engine fundamental. McGraw-Hill, (1988).
[2]   J.H. Horlock, D.E. Winterbone - Benson Rowland S. Thermodynamics and gas dynamics of Internal Combustion engine. New York: Clarendon Press Oxford (1986) Vol. II.
[3]   C.R. Ferguson and A.T. Kirkpatrick. Internal combustion engines. Second Edition, John Wiley and Sons, Inc. New York (2001).
[4]   H.N. Gupta and G. Prasad. Performance and emission prediction for a natural gas fueled spark-ignition engine. Proceedings of the XVI national conference on IC engines and combustion. Jan 20-22, (2000) pp. 230-235.
[5]   Maher A.R. Sadiq Al-Baghdadi, Haroun A.K. Shahad. Improvement of performance and reduction of pollutant emission of a four stroke spark ignition engine fueled with hydrogen-gasoline fuel mixture. Energy Conversion and Management 41 (2000) 77-91.
[6]   Maher A.R. Sadiq Al-Baghdadi. A simulation model for a single cylinder four- stroke spark ignition engine fueled with alternative fuels. Turkish J. Eng. Env. Sci. 30 (2006) 331-350.
[7]   J.V. Tirkey, H.N. Gupta, S.K. Shukla. Integrated Gas Dynamic and Thermodynamic Computational Modeling of Multicylinder 4-stroke SI engine using Gasoline as a fuel. Proceedings of 2008 ASME Summer Heat Transfer Conference HT2008, August 10-14, Jacksonville, Florida USA, (2008).
[8]   J.V. Tirkey, H.N. Gupta. Computer simulation and combustion diagnostic of multi cylinder 4-stroke SI engine using CNG as a fuel. International Journal of Applied Engineering Research (2008) Vol.3, No.5, pp. 667-680.
[9]   A. Agarwal and D.N. Assanis. Multi-Dimensional Modeling of Natural Gas Ignition under Compression Ignition Conditions Using Detailed Chemistry. SAE 980136, (1998).
[10] A. Agarwal, D. Assanis. Multi- Dimensional Modeling of Ignition, Combustion and Nitric Oxide Formation in Direct Injection Natural Gas Engines. SAE 2000-01-1839.
[11] R. Miller, G. Davis et al. A Super-Extended Zel'dovich Mechanism for NOX Modeling and Engine Calibration. SAE 980781, (1998).
[12] E. Sher and T. Bar-Kohany. Optimization of variable valve timing for maximizing performance of an unthrottled SI engine-a theoretical study. Energy 27 (2002) 757-775.
[13] Stephen R Turns. An Introduction to Combustion. 2nd ed. Singapore: McGraw-Hill; (2000).
[14] M.D. Checkel and J.D. Dale. Computerized knock detection from engine pressure records. SAE, 860028, (1986).

[15] K.M. Chun, J.B. Heywood. Characterization of knock in a spark ignition engine. SAE 890156, (1989).

[16] E. Moses, A.L. Yarin and P. Bar-Yoseph. On knocking prediction in spark ignition engines. Combustion and Flame 101: 239-261 (1995).

[17] A. By, B. Kempinski and J.M. Rife. Knock in spark ignition engines. SAE 810147, (1981).

[18] G. K?nig and C.G.W. Sheppard. End gas auto ignition phenomenon in internal combustion engine. SAE 902135, (1990).

[19] Soylu, J.V. Gerpen. Development of an auto ignition sub model for natural gas engines. Fuel 82(2003) 1699-1707.

[20] M.A. Liberman, M.F. Ivanov, O.E. Peil, D.M. Valiev and L.E. Eriksson. Numerical Modeling of the Propagating Flame and Knock Occurrence in Spark-Ignition Engines. Combust. Sci. and Tech., 177: 151-182, 2005.

[21] J.C. Livengood and P.C. Wu. Correlation of auto ignition phenomenon in internal combustion engine and rapid compression machines. Fifth symposium (International) on combustion, pp 347-356, 1955.

[22] A.M. Douaud and P. Eyzat. Four-octane number method for predicting the anti-knock behavior of fuels and engine. SAE 780080, 1978.

[23] C. Elmqvist, F. Lindstr?m and H.E. ?ngstr?m, B. Grandin, G. Kalghatgi. Optimizing Engine Concepts by Using a Simple Model for Knock Prediction. SAE 2003-01-3123.

[24] J.W.G. Turner et al. Performance and fuel economy enhancement of pressure charged SI engines through turboexpansion-An initial study. SAE 2003-01-0401.

[25] Seref Soylu. Prediction of knock limited operating conditions of a natural gas engine. Energy Conversion and Management 46 (2005) 121-138.

[26] M.U. Aslam, H.H. Masjuki et al. An experimental investigation of CNG as an alternative fuel for a retrofitted gasoline vehicle. Fuel 85 (2006) 717-724.

[27] Fanhua Ma, Yu Wang, Liu Haiquan, Y. Li, J. Wang, S. Zhao. Experimental study on thermal efficiency and emission characteristics of a lean burn hydrogen enriched natural gas engine. International Journal of Hydrogen Energy 32 (2007) 5067-5075.

[28] Rowland S. Benson. (Edited by Horlock JH, Winterbone DE) Thermodynamics and gas dynamics of Internal Combustion engine. New York: Clarendon Press Oxford 1982 Vol. I.

[29] W.J.D. Annand. Heat transfer in the cylinders of reciprocating internal combustion engine. Proc. Inst. Mech. Engrs. Vol.177, 973-990, (1963).

[30] A.N. Lipatnikov, J. Chomiak. Turbulent flame speed and thickness: phenomenology, evaluation, and application in multi-dimensional simulations. Progress in energy and combustion science 28 (2002) 1-74.

[31] S. Verhelst. and R. Sierens. A quasi-dimensional model for the power cycle of a hydrogen fueled ICE. International Journal of Hydrogen Energy 32 (2007) 3545-3554.

[32] S.Y. Liao, D.M. Jiang and Q. Cheng. Determination of laminar burning velocities for natural gas. Fuel 83(2004) 1247-1250.

[33] H.W. Branes-Moss. A designer's viewpoint, in passenger car engine. Conference Proceedings, Institution of Mechanical Engineers, London, 1975, pp. 133-47.

[34] G.H. Abd Alla. Computer simulation of a four stroke spark ignition engine. Energy Conversion and Management 43 (2002) 1043-1061.

[35] P.C. Baruah, R.S. Benson and H.N. Gupta. Performance and emission predictions for a multi-cylinder spark ignition engine with catalytic converter. SAE 780672, 1978.

[36] E. Zervas. Correlation between cycle-to-cycle variations and combustion parameters of a spark ignition engine. Applied Thermal Engineering. Vol. 24(2004) 2073-2081.

[37] M.A. Ceviz and F. Yüksel, Cyclic variation on LPG and Gasoline-fueled lean burn SI engine. Renewable Energy 31(2006) 1950-1960.

[38] J.C. Keck, J.B. Heywood, G. Noske. Early flame development and burning rates in spark ignition engines and their cyclic variability. SAE 870164, 1987.

[39] G.T. Kalghatgi. Spark ignition, Early flame development and cyclic variation in IC-Engines. SAE 870163, 1987.

Jeewan V. Tirkey is senior lecturer in Mechanical Engineering Department of IT BHU Varanasi, India. He has obtained his Ph.D. from BHU Varanasi in year 2008. His major research area is I.C.Engines. He has about 7 years of teaching and research experience.
Email address: jtirkey.mec@itbhu.ac.in

H.N. Gupta is a professor at Mechanical Engg. Deptt, IT BHU Varanasi India. He has obtained his Ph.D. from UK and working in the I.C.Engines field for about 20 years. He has many no. research papers including a book on I.C.Engines.

S.K. Shukla is basically a Mechanical Engineer with Master and Doctoral degree in Energy Systems from Indian Institute of Technology (I.I.T.) Delhi, India. Presently working as Reader in Thermal Engg., Department of Mechanical Engg., Institute of Technology, Banaras Hindu University(BHU), Varanasi, India. Author has more than 15 years of Industrial, Teaching and Research Experience. He has more than 21 no. of papers in journal and conference proceedings including ASME. Now He is working on a project sponsored by AICTE (Govt.of India), New Delhi, India.
E-mail address: skshukla.mec@itbhu.ac.in, Tel: 91-542-6702825, Fax: 91-542-2368157.